Acoustic and mechanical response of reservoir rocks under variable saturation and effective pressure

C. L. Ravazzoli[a)]
Facultad de Ciencias Astronómicas y Geofísicas, Universidad Nacional de La Plata, Paseo del Bosque, S/N, (1900) La Plata, Argentina

J. E. Santos
Facultad de Ciencias Astronómicas y Geofísicas, Universidad Nacional de La Plata, Paseo del Bosque, S/N, (1900) La Plata, Argentina, Department of Mathematics, Purdue University, 150 North University Street, West Lafayette, Indiana 47907-2068, and C.O.N.I.C.E.T., Argentina

J. M. Carcione
Istituto Nazionale di Oceanografia e di Geofisica Sperimentale (OGS), Borgo Grotta Gigante 42c, 34010 Sgonico, Trieste, Italy

(Received 24 May 2001; revised 15 September 2002; accepted 17 December 2002)

We investigate the acoustic and mechanical properties of a reservoir sandstone saturated by two immiscible hydrocarbon fluids, under different saturations and pressure conditions. The modeling of static and dynamic deformation processes in porous rocks saturated by immiscible fluids depends on many parameters such as, for instance, porosity, permeability, pore fluid, fluid saturation, fluid pressures, capillary pressure, and effective stress. We use a formulation based on an extension of Biot's theory, which allows us to compute the coefficients of the stress–strain relations and the equations of motion in terms of the properties of the single phases at the *in situ* conditions. The dry-rock moduli are obtained from laboratory measurements for variable confining pressures. We obtain the bulk compressibilities, the effective pressure, and the ultrasonic phase velocities and quality factors for different saturations and pore-fluid pressures ranging from normal to abnormally high values. The objective is to relate the seismic and ultrasonic velocity and attenuation to the microstructural properties and pressure conditions of the reservoir. The problem has an application in the field of seismic exploration for predicting pore-fluid pressures and saturation regimes. [DOI: 10.1121/1.1554696]

PACS numbers: 43.20.Jr, 43.20.Hq [ANN]

I. INTRODUCTION

Rock-acoustic models relating the petrophysical characteristics of rocks—and their pore fluids at *in situ* conditions—with the acoustic properties, are essential tools in reservoir geophysics. Important applications are time-lapse seismics, geomechanics of petroleum-rich rocks, and reservoir characterization, evaluation, and monitoring.

The fundamental concepts about the stress–strain relations and the dynamics of porous deformable rocks fully saturated by single-phase fluids were established in the pioneer works of Biot.[1–3] However, when the pore volume is occupied by more than one fluid phase, a different treatment is required, depending on the behavior of the fluids and their distribution within the pore space. Theoretical formulations for the study of the deformation and wave propagation in porous rocks with partial, miscible, or segregated fluid saturation have been presented by different authors. In this regard, Dutta and Odé[4] analyzed the attenuation and dispersion of seismic waves in a brine-saturated rock containing spherical gas pockets using a model based on Biot's equations and White's model.[5] Another application of Biot's formulation was presented by Mochizuki[6] to analyze experimental data in partially saturated rocks. The two fluids were modeled as a single phase one by means of a volume average for the density, an apparent viscosity, and an effective fluid compressibility. Some years later, using variational principles, Berryman *et al.*[7] derived a theory for wave propagation in porous rocks saturated by segregated fluids (liquid and gas) and also for the case of mixing of liquid and gas. A different approach, based on a scattering theory, was employed by Toksöz *et al.*[8] for pores of different shapes to analyze seismic velocities for variable pressure and saturation conditions. In this model two phase fluids are treated as inclusions (miscible or immiscible) and is also valid when each fluid occupies different parts of the pore space.

It must be remarked that none of these models incorporate the capillary forces existing when two immiscible fluids share the same pore volume. To take this effect into account, Santos *et al.*[9,10] developed a theory based on a Lagrangian formulation and the principle of virtual complementary work. Consequently, unlike the previously mentioned models, this theory takes into account the residual saturations of both fluid phases and the fact that pressure variations induced by wave propagation are different in the two fluid phases. Some applications of this model were recently pub-

a)Electronic mail: claudia@fcaglp.fcaglp.unlp.edu.ar; fax: 0054 221 4236591.

lished in Refs. 11, 12 for the estimation of gas hydrate concentration and free gas saturation from well logs and seismic data. Also, an interesting analysis and discussion about this subject was presented by Corapcioglu.[13]

In recent years, the oil industry has shown an increasing interest in the use of high-frequency seismic data for studying the changes in pore pressure and poroelastic moduli during production. Of utmost importance is the determination of fluid saturation and its distribution, and the pressure regime of the hydrocarbon fluids before drilling, since the prediction and detection of rocks with abnormally high fluid pressures (*overpressure*) is important to minimize risks and avoid dangerous blowouts during drilling operations. The occurrence of overpressure phenomena is observed in sedimentary basins worldwide and is associated with different mechanisms.[14] The most important are gas to oil conversion (cracking)[15] and disequilibrium compaction.[16]

In connection with these subjects, our main objective in this work is to present the application of a generalized version of the model described in Refs. 9, 10 to analyze the mechanical and acoustical properties of a consolidated reservoir sandstone saturated by immiscible fluids under variable confining and fluid pressures.

Ultrasonic laboratory experiments on dry samples[17] for different confining pressures provide the dry-rock moduli versus effective pressure. These moduli and the effective stress coefficients are the most important parameters, since they characterize the acoustic properties of the rock. Our results indicate that the model is suitable for studying the transition zones within hydrocarbon reservoirs, providing a unified relationship between the properties of the rock frame and the pore fluids and their static and dynamic responses.

The paper is organized as follows. In Sec. II, we give the generalities of the model and a brief review of definitions and concepts regarding compressibilities and effective pressure. In the next section, we describe the equations of motion, the elastic coefficients of the model, and the propagation of elastic waves in a porous isotropic rock saturated by immiscible fluids, and give expressions for the phase velocities and quality factors. In Sec. IV, we apply the previous formulation to analyze the effects of variable saturation and fluid pressures on bulk compressibilities, effective pressure, phase velocities, and quality factors. We consider fluid pressures ranging from the normal hydrostatic state to abnormally high values, close to the fracturing limit. We use a realistic capillary pressure curve, and frequency-dependent dissipation, satisfying appropriate thermodynamic conditions.

II. BULK COMPRESSIBILITIES AND EFFECTIVE PRESSURE OF A THREE PHASE MEDIUM

Let us consider a volume V_b of a porous medium fully saturated by two immiscible fluids (such as oil, brine, or free gas) under a confining pressure P_c. In these situation, the distribution of fluids in the pore space depends on the wettability of the rock, i.e., its relative preference to be covered by a certain phase. The fluid in contact with the pore surface is the so-called wetting phase. In the following, the subscripts "w" and "n" refer to the wetting and nonwetting fluids, respectively. Then, we denote S_w and S_n the averaged wetting and nonwetting fluid saturations, respectively, which are assumed to satisfy the condition of complete pore volume saturation: $S_n+S_w=1$. The model assumes that both fluids can flow in the pore space, and, consequently, we only consider saturation states within the range[18–21]

$$S_{rn}<S_n<1-S_{rw}, \quad S_{rw}<S_w<1-S_{rn}, \tag{2.1}$$

where S_{rn} and S_{rw} denote the residual saturations of both phases. The saturation S_{rn} is the amount of nonwetting fluid that remains in the pore space when the capillary pressure tends to zero, and S_{rw}—also called irreducible saturation—is the remaining wetting fluid when the capillary pressure reaches its maximum value.

Let ΔP_n, ΔP_w, and ΔS_n denote, respectively, infinitesimal changes in the pressures of the nonwetting and wetting fluids and the nonwetting fluid saturation, with respect to corresponding reference values $\overline{P}_n$, $\overline{P}_w$, and $\overline{S}_n$ associated with the initial equilibrium state. Recall that the fluid pressures are related through the capillary relation[18,20,21]

$$\begin{aligned} P_{ca}(S_n)=P_{ca}(\overline{S}_n+\Delta S_n)&=\overline{P}_n-\overline{P}_w+\Delta P_n-\Delta P_w \\ &=P_{ca}(\overline{S}_n)+\Delta P_{ca}. \end{aligned} \tag{2.2}$$

Based on experimental data and ignoring hysteresis, we will assume that P_{ca} is a positive and strictly increasing function of the nonwetting fluid saturation.

Next, using some formulas given by Santos *et al.*,[10] we will define and compute the bulk compressibilities for this type of media using a generalization of the arguments given by Zimmerman[22] for single-phase fluids. First, from the strain–stress relations in that formulation we obtain an expression of the specific change in bulk volume $e_b=\Delta V_b/\overline{V}_b$ from a reference undeformed state $\overline{V}_b$ due to changes in P_c, P_w, and P_n. Thus, from (39), (41a) and the expressions for $(3D^*+1/2N)$, F_1, F_2 in Ref. 10 and applying the capillary relation (2.2), it can be shown that[23]

$$e_b=-C_m\Delta P_c-\delta(\overline{S}_n+\beta)\Delta P_n-\delta(\overline{S}_w-\beta)\Delta P_w, \tag{2.3}$$

where $\delta=C_s-C_m$, C_s and C_m being the compressibilities of the solid grains and dry matrix, $\beta=P_{ca}(\overline{S}_n)/P'_{ca}(\overline{S}_n)$ and $P'_{ca}(\overline{S}_n)=dP_{ca}/dS_n$.

Since the variations of the bulk volume V_b are due to the changes of three different pressures that may vary independently, we can define the following bulk compressibilities:

$$C_{bc}=-\frac{1}{\overline{V}_b}\left(\frac{\Delta V_b}{\Delta P_c}\right)_{P_w,P_{ca}}=\frac{1}{K_m}=C_m, \tag{2.4}$$

$$C_{bw}=\frac{1}{\overline{V}_b}\left(\frac{\Delta V_b}{\Delta P_w}\right)_{P_c,P_{ca}}=C_m-C_s, \tag{2.5}$$

$$C_{bca}=\frac{1}{\overline{V}_b}\left(\frac{\Delta V_b}{\Delta P_{ca}}\right)_{P_c,P_w}=(\overline{S}_n+\beta)(C_m-C_s), \tag{2.6}$$

where $K_m=C_m^{-1}$ is the bulk modulus of the dry matrix. The first two compressibilities are completely analogous to those

of the single-phase fluid case. In particular, (2.5) shows that P_w plays the same role as the "pore pressure" P_p used in the single-phase case.[22]

Next, combining (2.4)–(2.6) and the capillary relation (2.2), Eq. (2.3) can be rewritten in differential form as follows:

$$e_b = -C_{bc}(P_c,P_w,P_{ca})dP_c + C_{bw}(P_c,P_w,P_{ca})dP_w + C_{bca}(P_c,P_w,P_{ca})dP_{ca}. \tag{2.7}$$

Assuming that e_b is an exact differential of the variables P_c, P_w, and P_{ca} and that C_s is constant, from (2.4), (2.5), and (2.7), we get

$$C_{bc} = C_{bc}(P_c - P_w, P_{ca}), \tag{2.8}$$

and from (2.6) and (2.7),

$$C_{bca} = C_{bca}(P_c - P_w, P_{ca}) = (\overline{S}_n + \beta)(C_{bc}(P_c - P_w, P_{ca}) - C_s), \tag{2.9}$$

Next, following Zimmerman,[22] to obtain an effective pressure law for bulk volume deformation we compute the total strain E_b, integrating (2.7) in the (P_c,P_w,P_{ca}) state variables, along the following paths:

Path 1: $(0,0,P_{ca}(S_n^*)) \rightarrow (P_c,0,P_{ca}(S_n^*))$,

Path 2: $(P_c,0,P_{ca}(S_n^*)) \rightarrow (P_c,\overline{P}_w,P_{ca}(S_n^*))$,

Path 3: $(P_c,\overline{P}_w,P_{ca}(S_n^*)) \rightarrow (P_c,\overline{P}_w,P_{ca}(\overline{S}_n))$,

obtaining

$$E_b = \int_0^{P_c} e_b\,dp_1 + \int_0^{\overline{P}_w} e_b\,dp_2 + \int_{P_{ca}(S_n^*)}^{P_{ca}(\overline{S}_n)} e_b\,dp_3 \simeq -\overline{C}_{bc}(P_c - \overline{P}_w, P_{ca}(S_n^*))P_{\mathrm{ef}}^b, \tag{2.10}$$

resulting in a *bulk effective pressure law* P_{ef}^b given by

$$P_{\mathrm{ef}}^b = P_c - \overline{n}_{b1}\overline{P}_w - \overline{n}_{b2}(P_{ca}(\overline{S}_n) - P_{ca}(S_n^*)), \tag{2.11}$$

where

$$\overline{n}_{b1} = 1 - C_s/\overline{C}_{bc}(P_c - \overline{P}_w, P_{ca}(S_n^*)), \tag{2.12}$$

$$\overline{n}_{b2} = \overline{C}_{bca}(P_c - \overline{P}_w, P_{ca}(S_n^*), P_{ca}(\overline{S}_n))/\overline{C}_{bc}(P_c - \overline{P}_w, P_{ca}(S_n^*)). \tag{2.13}$$

It must be observed that the integration in the capillary pressure variable (Path 3) does not begin at $P_{ca}=0$ since such a value corresponds to the irreducible saturation S_{rn}. To avoid loss of generality we start the process at an arbitrary saturation S_n^* within the range (2.1).

The coefficients $\overline{C}_{bca}$ and $\overline{C}_{bc}$, are the mean (or "secant") values of the compressibilities C_{bca} and C_{bc} in the intervals $[0,P_c]$ and $[P_{ca}(S_n^*),P_{ca}(\overline{S}_n)]$, respectively,

$$\overline{C}_{bc}(P_c,P_{ca}(\overline{S}_n)) = \frac{1}{P_c}\int_0^{P_c} C_{bc}(p,P_{ca}(\overline{S}_n))dp, \tag{2.14}$$

$$\begin{aligned}\overline{C}_{bca}(P_c - \overline{P}_w, P_{ca}(S_n^*), P_{ca}(\overline{S}_n)) &= \frac{1}{P_{ca}(\overline{S}_n) - P_{ca}(S_n^*)}\int_{P_{ca}(S_n^*)}^{P_{ca}(\overline{S}_n)} C_{bca}(P_c - \overline{P}_w, p_3)dp_3 \\ &= \frac{1}{P_{ca}(\overline{S}_n) - P_{ca}(S_n^*)}\int_{S_n^*}^{\overline{S}_n}[s+\beta(s)] \\ &\quad \times [C_{bc}(P_c - \overline{P}_w, P_{ca}(s) - C_s]P'_{ca}(s)ds,\end{aligned} \tag{2.15}$$

where we have used (2.6) and the fact that $p_3 = p_3(s)$ is the capillary pressure function and the variable s takes values in the saturation range $[S_n^*,\overline{S}_n]$.

It must be remarked that the effective pressure in this case not only depends on the confining and wetting fluid pressures but also on the changes in capillary pressure.

III. EQUATIONS OF MOTION AND ELASTIC COEFFICIENTS

In this section we present the equations of motion for this kind of media, which will be used in Sec. IV to compute seismic wave velocities and quality factors. Our objective is to analyze the combined effects of saturation and confining and pore pressures on the properties of the different wave modes.

Let $\mathbf{u}^s$, $\tilde{\mathbf{u}}^n$, and $\tilde{\mathbf{u}}^w$ denote the time Fourier transforms of the averaged absolute displacements for the solid, nonwetting, and wetting fluid phases, respectively. If ϕ denotes the effective porosity, then we introduce the relative fluid displacements $\mathbf{u}^n$ and $\mathbf{u}^w$, given by $\mathbf{u}^l = \phi(\tilde{\mathbf{u}}^l - \mathbf{u}^s)$, $l = n,\ w$.

For a spatially homogeneous medium, the frequency–domain equations of motion take the following form:

$$\begin{aligned}(i)\quad & -\omega^2(\rho\mathbf{u}^s + \rho_n\overline{S}_n\mathbf{u}^n + \rho_w\overline{S}_w\mathbf{u}^w) \\ &= (K_c + \tfrac{4}{3}N)\boldsymbol{\nabla}(\boldsymbol{\nabla}\cdot\mathbf{u}^s) - N\boldsymbol{\nabla}\times\boldsymbol{\nabla}\times\mathbf{u}^s + B_1(\boldsymbol{\nabla}\cdot\mathbf{u}^n) \\ &\quad + B_2\boldsymbol{\nabla}(\boldsymbol{\nabla}\cdot\mathbf{u}^w); \\ (ii)\quad & -\omega^2(\rho_n\overline{S}_n\mathbf{u}^s + g_n\mathbf{u}^n + g_{nw}\mathbf{u}^w) + i\omega\, d_n\mathbf{u}^n - i\omega\, d_{nw}\mathbf{u}^w \\ &= B_1\boldsymbol{\nabla}(\boldsymbol{\nabla}\cdot\mathbf{u}^s) + M_1\boldsymbol{\nabla}(\boldsymbol{\nabla}\cdot\mathbf{u}^n) + M_3\boldsymbol{\nabla}(\boldsymbol{\nabla}\cdot\mathbf{u}^w); \\ (iii)\quad & -\omega^2(\rho_w\overline{S}_w\mathbf{u}^s + g_{nw}\mathbf{u}^n + g_w\mathbf{u}^w) + i\omega\, d_w\mathbf{u}^w - i\omega\, d_{nw}\mathbf{u}^n \\ &= B_2\boldsymbol{\nabla}(\boldsymbol{\nabla}\cdot\mathbf{u}^s) + M_3\boldsymbol{\nabla}(\boldsymbol{\nabla}\cdot\mathbf{u}^n) + M_2\boldsymbol{\nabla}(\boldsymbol{\nabla}\cdot\mathbf{u}^w),\end{aligned} \tag{3.1}$$

where $\omega = 2\pi f$ denotes the angular frequency and f is the frequency. The coefficients ρ_n and ρ_w are the mass densities of the fluids and ρ is the mass density of the bulk material, which is related to the grain density ρ_s and the porosity as

$$\rho = (1-\phi)\rho_s + \phi(\overline{S}_n\rho_n + \overline{S}_w\rho_w). \tag{3.2}$$

The quantities g_n, g_w, g_{nw}, are mass coupling coefficients; as in the classical Biot's theory for single-phase fluid saturation, they represent the inertial effects associated with dynamic interactions between the three different phases. The coefficients d_n, d_w, and d_{nw} represent viscous drag effects that can be expressed in terms of the viscosities and relative permeabilities of each fluid phase.

For frequencies higher than characteristic frequencies to be defined later, these coefficients need to be modified. For simple pore geometries like plane slits and cylindrical ducts Auriault *et al.*[24] gave explicit expressions for frequency-dependent relative permeability tensors using homogenization techniques. In Sec. IV we will define the mass and viscous coupling coefficients using an extension of the ideas described in Refs. 2 and 25.

The elastic moduli K_c, B_1, B_2, M_1, M_2, M_3 are given by the following formulas that can be obtained with the arguments given in Ref. 10 and taking into account the reference pressures $\overline{P}_w$, $\overline{P}_n$ of both fluid phases:

$$K_c=\frac{K_s(K_m+\Xi)}{(K_s+\Xi)},\quad \Xi=\frac{K_f(K_m-K_s)}{\phi(K_f-K_s)},$$

$$K_f=\alpha\left(\frac{\gamma\overline{S}_n}{K_n}+\frac{\overline{S}_w}{K_w}\right)^{-1},\quad \alpha=1+(\overline{S}_n+\beta)(\gamma-1), \tag{3.3}$$

$$\gamma=\left(1+\frac{P'_{ca}(\overline{S}_n)\overline{S}_n\overline{S}_w}{K_w}\right)\left(1+\frac{P'_{ca}(\overline{S}_n)\overline{S}_n\overline{S}_w}{K_n}\right)^{-1}.$$

The remaining coefficients can be obtained by using the following relations:

$$\begin{aligned}
&B_1=\chi K_c[(\overline{S}_n+\beta)\gamma-\beta+(\gamma-1)\zeta],\\
&B_2=\chi K_c[(\overline{S}_w+(1-\gamma)\zeta],
\end{aligned} \tag{3.4}$$

$$\begin{aligned}
&M_1=-M_3-\frac{B_1}{\delta K_m},\quad M_2=\frac{r}{q}B_2+\frac{\zeta}{q},\\
&M_3=-B_2\left[\frac{r}{q}+\frac{1}{K_m\delta}\right]-\frac{\zeta}{q},
\end{aligned} \tag{3.5}$$

with

$$\chi=\left[\delta+\phi\left(\frac{1}{K_m}-\frac{1}{K_c}\right)\right]\left\{\alpha\left[\delta+\phi\left(\frac{1}{K_m}-\frac{1}{K_f}\right)\right]\right\}^{-1},$$

$$r=\frac{\overline{S}_n+\beta}{K_s}+\frac{1}{K_c-K_m}\left[qB_2+(\overline{S}_n+\beta)\left(1-\frac{K_c}{K_s}\right)\right],$$

$$q=\phi\left(\frac{1}{K_n}+\frac{1}{P'_{ca}\overline{S}_n\overline{S}_w}\right),$$

where $\zeta=\overline{P}_w/P'_{ca}(\overline{S}_n)$. According to Gassman's theory,[26] it will be assumed that the coefficient N is identical to the shear modulus of the dry rock N_m.

It is known that wave dispersion and attenuation in real saturated porous media is higher than that predicted by Biot-type theories, in which dissipation is mainly due to viscodynamic effects. The main discrepancies are related to the complexity of the pore shapes, heterogeneities in the spatial distribution of the fluids, and other physical properties, the presence of clays and the anelasticity of the rock matrix. These factors give rise to a variety of attenuation mechanisms that can be included in the formulation, introducing viscoelasticity. The resultant poroviscoelastic moduli are complex and frequency-dependent functions and their computation will be explained in detail in Sec. IV C.

TABLE I. Properties of Bandera sandstone.

Porosity, ϕ	20%
Absolute permeability, K	3.5×10^{-15} m^2
Grain density, ρ_s	2700 kg/m^3
Grain bulk modulus, K_s	44 GPa

The plane wave analysis performed in Ref. 9 shows that in these types of media, three different compressional waves (Type I, Type II, and Type III) and one shear wave (or S wave) propagate.

The Type-I wave is the analog of the classical fast P wave propagating in elastic or viscoelastic isotropic solids and is associated with the motion of both solid and fluids moving nearly in phase. Type II and Type III are slow waves strongly attenuated in the low-frequency range. The first one is analogous to the classical Biot's slow wave, with the two fluids moving nearly in phase and in opposite phase with the solid. For the Type-III waves, both fluids move in nearly opposite phase with each other.

Denoting by k_j, $j=$I, II, III, S, the complex wave numbers, the phase velocities C_j and quality factors Q_j are obtained by using the formulas

$$C_j=\frac{\omega}{\mathrm{Re}(k_j)},\quad Q_j=-\frac{1}{2}\frac{\mathrm{Re}(k_j)}{\mathrm{Im}(k_j)},\quad j=\mathrm{I,II,III,S}. \tag{3.6}$$

IV. APPLICATION TO THE STUDY OF REAL SANDSTONES

In this section, we apply the theoretical formulation described in previous sections to predict and investigate the behavior of the compressibilities, wave velocities, and quality factors of hydrocarbon reservoir rocks at *in situ* conditions. We use the ultrasonic laboratory data published by King,[17] who measured compressional and shear wave velocities of a set of sandstones (dry and fully saturated) under variable confining pressure. Among the available samples, we chose *Bandera* sandstone, a well-cemented and consolidated feldespathic graywacke.[27] The petrophysical and geotechnical characteristics of the sample (porosity, permeability, grain density, and bulk modulus) are taken from King[17] and Mann and Fatt[27] (see Table I). The mineral bulk modulus K_s is taken from Zimmerman.[22] The sandstone is assumed to be isotropic.

To introduce the variation of the matrix properties with effective pressure, we obtained the dependence of the (elastic) shear and bulk dry-rock moduli $N_m(P_c)$ and $K_m(P_c)$ versus confining pressure. For that purpose, we assume that for each P_c, the measured velocities can be described in terms of the simplified elastic isotropic approximation. Then, we performed exponential regressions of the form

$$\begin{aligned}
f^{-1}(P_c)=&y_0+A_1\exp(-(P_c-P_0)/t_1)\\
&+A_2\exp(-(P_c-P_0)/t_2),
\end{aligned} \tag{4.1}$$

where f stands for N_m or K_m. The coefficients are given in Table II.

Since fluid pressure for a dry sample can be assumed to be zero, the effective pressure equals the confining pressure.

TABLE II. Coefficients of Eq. (4.1) for Bandera sandstone. For pressures given in MPa the moduli result in GPa.

	P_0	y_0	A_1	t_1	A_2	t_2
$(K_m)^{-1}$	2.318 591 921 065	7.9435×10^{-2}	8.687×10^{-2}	3.509	8.553×10^{-2}	19.32
$(N_m)^{-1}$	1.524 982 994 273	7.9698×10^{-2}	3.342×10^{-2}	8.22	1.956×10^{-2}	41.26

Then, to obtain the elastic properties of the skeleton for a given combination of confining and fluid pressures, we simply replace P_c by the effective pressure P_{ef}^b [given by (2.11)] in Eq. (4.1). The whole set of poroelastic moduli are then computed using (3.3)–(3.5).

The mass and viscous coupling coefficients in the equations of motion (3.1) are computed by using the expressions given in Ref. 9 modified by frequency correction factors:

$$g_l(\omega)=\frac{F_s\rho_l\overline{S_l}}{\phi}+\mu_l(\overline{S_l})^2D_l\frac{F_I(\theta_l)}{\omega},\quad l=n,\omega; \tag{4.2}$$

$$g_{nw}(\omega)=\epsilon\frac{F_s}{\phi}(\rho_n\rho_w,\overline{S_n},\overline{S_w})^{1/2} + \frac{(\mu_n\mu_w)^{1/2}\overline{S_n}\,\overline{S_w}k_{rnw}}{D}\frac{F_I(\theta_{nw})}{\omega}; \tag{4.3}$$

$$d_l(\omega)=\mu_l(\overline{S_l})^2D_lF_R(\theta_l),\quad l=n,\omega; \tag{4.4}$$

$$d_{nw}(\omega)=\frac{(\mu_n\mu_w)^{1/2}\overline{S_n}\,\overline{S_w}k_{rnw}}{D}F_R(\theta_{nw}); \tag{4.5}$$

where $D=K(k_{rn}k_{rw}-k_{rnw}^2)$, $D_n=k_{rw}/D$, $D_w=k_{rn}/D$. The constants μ_n, μ_w are the fluid viscosities and K, $k_{rn}(S_n)$, $k_{rw}(S_n)$ and $k_{rnw}(S_n)$ are the absolute and coupling permeability functions, respectively. The relative permeability functions and the capillary pressure $P_{ca}(S_n)$ used here are computed using the relations[28]

$$k_{rn}(S_n)=\left(1-\frac{1-S_n}{1-S_{rn}}\right)^2,\quad k_{rw}(S_n)=\left(\frac{1-S_n-S_{rw}}{1-S_{rw}}\right)^2, \tag{4.6}$$

$$P_{ca}(S_n)=A\left(\frac{1}{(S_n+S_{rw}-1)^2}-\frac{S_{rn}^2}{S_n^2(1-S_{rn}-S_{rw})^2}\right). \tag{4.7}$$

Also, we take $k_{rnw}(S_n)=\sqrt{\epsilon k_{rn}(S_n)k_{rw}(S_n)}$. These relations are based on laboratory experiments performed on different porous rocks during imbibition and drainage processes (neglecting hysteresis effects). However, it must be pointed out that those functions depend on the nature of the porous medium and the wettability of the pore fluids involved. In what follows the capillary pressure amplitude coefficient A equals 3 KPa. The residual saturation values are $S_{rn}=S_{rw}=5\%$ and, consequently, the saturation S_n in all the calculations varies in the range

$$0.06\leqslant\overline{S_n}\leqslant0.94. \tag{4.8}$$

The factor ϵ in the definition of k_{rnw} is taken to be 0.01. The parameter F_s is the formation structure factor and is related to the tortuosity of the pores. It can be estimated using the following relation:[29] $F_s=1/2(1+1/\phi)$.

The complex-valued frequency-dependent function $F(\theta_j)=F_R(\theta_j)+iF_I(\theta_j)$, $j=n$, w, nw in (4.2)–(4.5) is the "universal" frequency correction function defined by Biot[2] for single-phase fluids:

$$F(\theta)=\frac{1}{4}\frac{\theta T(\theta)}{1-\frac{2}{i\theta}T(\theta)},\quad T(\theta)=\frac{\mathrm{ber}'(\theta)+i\,\mathrm{bei}'(\theta)}{\mathrm{ber}(\theta)+i\,\mathrm{bei}(\theta)},$$

with $\mathrm{ber}(\theta)$ and $\mathrm{bei}(\theta)$ being the Kelvin functions of the first kind and zeroth order. The arguments θ_j for $F(\theta_j)$, $j=n$, w, nw in (4.2)–(4.5) can be estimated as in Refs. 2 and 25,

$$\theta_j=a_p^j\sqrt{\frac{\omega\rho_j}{\mu_j}},\quad a_p^j=2\sqrt{\frac{Kk_{rj}A_0}{\phi}},\quad j=n,w,nw, \tag{4.9}$$

where A_0 denotes the Kozeny–Carman constant.[18,30] This correction function $F(\theta)$ is needed for frequencies higher than the minimum of the characteristic frequencies, defined as

$$\omega_c^l(\overline{S_n})=\frac{\overline{S_l}\mu_l\phi D_l}{F_s\rho_l},\quad l=n,w,$$
$$\omega_c^{nw}(\overline{S_n})=\frac{\phi(\mu_n\mu_w)^{1/2}(\overline{S_n}\,\overline{S_w})^{1/2}k_{rnw}}{\epsilon DF_s(\rho_n\rho_w)^{1/2}}. \tag{4.10}$$

These expressions have been obtained, taking into account that we have two immiscible fluids and three relative permeability functions, following the ideas given in Ref. 7 for the case of segregated fluids.

In the following numerical tests, we study the mechanical response of the sandstone saturated by brine (the wetting phase) and oil (nonwetting phase) at a fixed confining pressure (i.e., at a fixed depth), for variable fluid pressures and saturation states. The model represents a transition zone within a hydrocarbon reservoir. We assume that the rock is located at a depth of about 3000 m at a confining pressure of about 70 MPa. The physical properties of brine and oil—assumed to be independent of pressure—are presented in Table III.

A. Effective pressure law

It is a well-established fact that knowledge of the effective pressure law of a porous saturated rock is essential for the study of its mechanical behavior. In many cases, it has

TABLE III. Physical properties of brine and oil.

Fluid	Density	Viscosity	Bulk modulus
Brine	1030 kg/m^3	0.001 N s/m^2	2.25 GPa
Oil	700 kg/m^3	0.01 N s/m^2	0.57 GPa

been observed that when both confining and formation fluid pressures change, only the difference between the two, i.e., the *differential pressure*, has a significant effect on elastic properties and velocities. In particular, when this difference is small, the differential pressure gives a reasonable estimate of the effective pressure.[31] Since in our model we have two different fluid pressures that can vary independently, such a comparison cannot be directly done. Instead, we introduce two differential pressures, associated with each fluid phase, namely

$$P_{wd}=P_c-\overline{P}_w, \quad P_{nd}=P_c-\overline{P}_n. \tag{4.11}$$

As stated in the Introduction, we are interested in the study of acoustic wave propagation in overpressured formations. Such a physical condition of the rock is commonly quantified in terms of an ''excess pore pressure,'' defined as the difference between the fluid pressure and the hydrostatic pressure P_h exerted by a column of water extending from the surface up to the depth under consideration. Thus, we define the excess pressure of each fluid phase as

$$\Delta P_{wh}=\overline{P}_w-P_h, \quad \Delta P_{nh}=\overline{P}_n-P_h. \tag{4.12}$$

In the following numerical tests, the wetting fluid pressure $\overline{P}_w$ (analogous to ''pore pressure'') is varied from the water hydrostatic pressure P_h for the considered depth (about 29 MPa) to the confining pressure value, assuming that the wetting fluid pressure cannot exceed the confining pressure.

To obtain the coefficients $\overline{n}_{b1}$ and $\overline{n}_{b2}$ given by Eqs. (2.12) and (2.13), we first estimate the secant compressibilities $\overline{C}_{bc}$ and $\overline{C}_{bca}$, disregarding the possible dependence of the C_{bc} coefficient on P_{ca}. The initial saturation state in these computations is $S_n^*=0.053$. Next, using Eq. (2.11), we obtain the effective pressure law for the deformation of the bulk volume $P_{\mathrm{ef}}^b(P_c,\overline{P}_w,P_{ca}(\overline{S}_n))$ for each fluid pressure and saturation state. The effective pressure law is then analyzed as a function of the wetting fluid pressure and saturation.

Figure 1(a) shows the resulting P_{ef}^b versus wetting fluid pressure for $\overline{S}_n=0.4$ (at constant $P_{ca}\approx 10$ KPa). We compare the results of our model with other possible estimates, such as the wetting-differential pressure P_{wd} and a general law proposed by Gangi and Carlson[31] of the form

$$P_{\mathrm{ef}}^b=P_c-n_G\overline{P}_w, \quad \text{with } n_G=n_0-n_1P_{wd}. \tag{4.13}$$

In these equations, the ''pore pressure'' is replaced by its equivalent $\overline{P}_w$, and we have considered $n_0=1$ and $n_1=0.014\ \mathrm{MPa}^{-1}$, with pressures given in MPa.

For a fixed saturation, we observe significant differences, particularly in the low pore pressure range. As expected, the increase in wetting fluid pressure causes a reduction in the effective pressure acting on the solid matrix, which produces a ''softening'' effect in the formation. Thus, the behavior of the effective pressure law is consistent with the previously defined laws and explains the well-known effect of the decreasing of seismic velocities observed in overpressured formations.

Figure 1(b) shows the effect of changes in saturation—and therefore capillary pressure—on the effective pressure

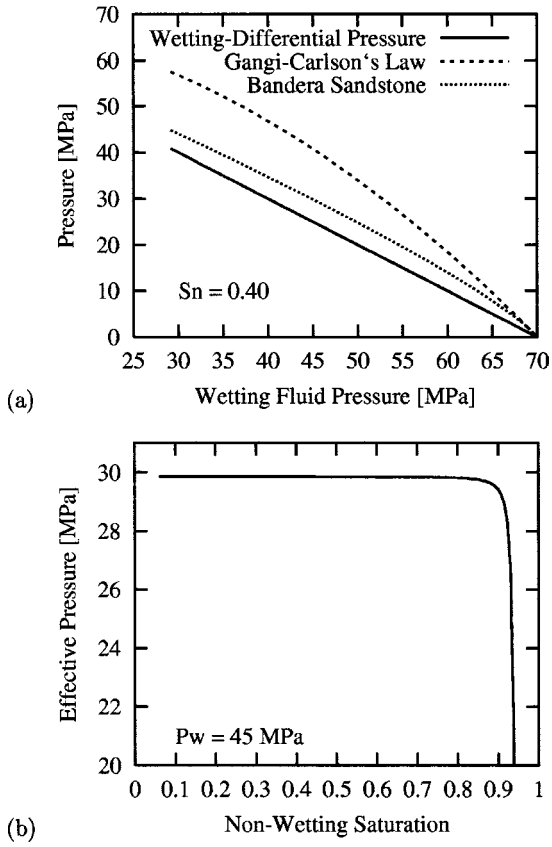

FIG. 1. (a) A comparison of effective pressure, wetting-differential pressure (P_w^d), and Gangi–Carlson's law for $\overline{S}_n=0.40$. (b) Effective pressure versus saturation $\overline{S}_n$ (increasing P_{ca}) for $\overline{P}_w=45$ MPa and $P_c=70$ MPa.

law, keeping the wetting fluid pressure $\overline{P}_w$ constant at 45 MPa. Although the effective pressure is almost independent of $\overline{S}_n$, a marked decrease can be appreciated (of about 33%) when $\overline{S}_n$ approaches its upper limit, i.e., near the residual brine saturation. This reduction also depends on confining and wetting fluid pressures and is associated with the rapid growth of the capillary pressure and the $\overline{n}_{b2}$ coefficient. The behavior of the effective pressure coefficients versus pressure and saturation is shown in Figs. 2(a) and (b), respectively. In the first plot, we observe that when $\overline{P}_w$ approaches P_c (i.e., near the fracture limit) $n_{b1}\to 1$ and $n_{b2}\to 0$, and $P_{\mathrm{ef}}^b\to P_{wd}$. This is due to the asymptotic limit of the compressibility $\overline{C}_{bc}$ that tends to infinity for $\overline{P}_w\to P_c$.

It is worthwile to remark that, when considering elastic wave propagation in this kind of media, the different wave modes induce infinitesimal oscillatory changes in the stresses and pressures of the solid and fluid phases with respect to their reference equilibrium values. Under this assumption the stress–strain process takes place within the linear range. However, those increments are not taken into account in the evaluation of the effective pressure law, which is computed in terms of P_c, $\overline{P}_w$, and $P_{ca}(\overline{S}_n)$.

B. Bulk compressibilities versus saturation and pressure

In this section, we apply the equations given in Sec. II to compute the bulk compressibilities of the sandstone. A simi-

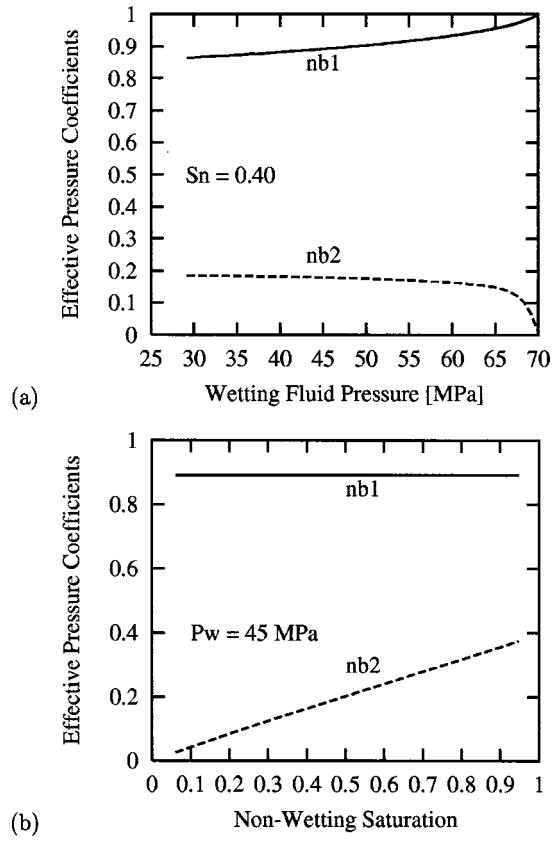

FIG. 2. Effective pressure coefficients n_{b1} and n_{b2} (a) versus pore pressure $\overline{P_w}$ (for $\overline{S_n}=0.40$), (b) versus saturation $\overline{S_n}$ (increasing P_{ca}) for $\overline{P_w}=45$ MPa.

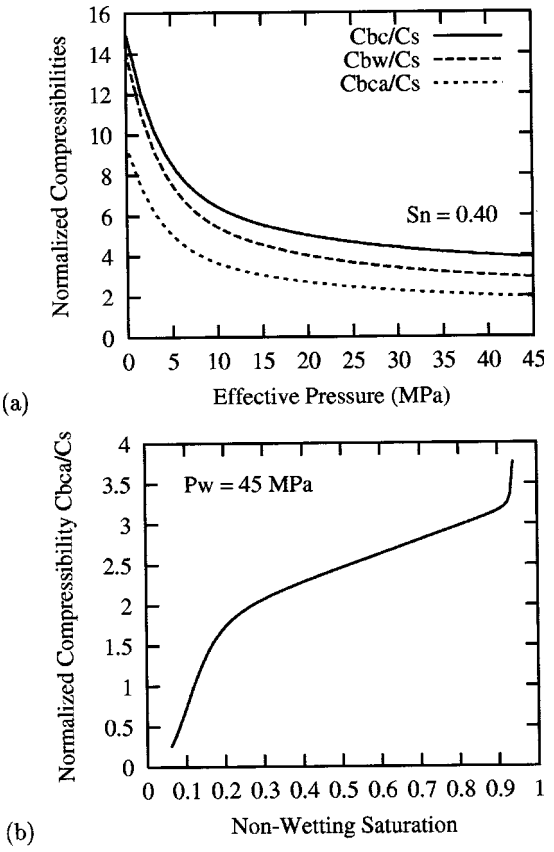

FIG. 3. (a) Normalized compressibilities C_{bc} $(=C_m)$, C_{bw} and C_{bca} of Bandera sandstone versus bulk effective pressure; (b) C_{bca} versus nonwetting fluid saturation.

lar analysis was presented in Ref. 32. To estimate the elastic response for different combinations of the state variables, using the law (4.1) previously obtained for $K_m(P_c)$, we evaluate the coefficient $C_m=K_m^{-1}$ at each effective pressure. In this way, we obtain the variation of the compressibilities (2.4)–(2.6) with effective pressure, assuming constant grain compressibility C_s and an elastic reversible behavior. As pointed out in Ref. 33, this is valid for well-cemented and consolidated rocks, but in loose unconsolidated sands the compaction is both anelastic and irreversible.

Figure 3(a) shows the compressibilities C_{bc}, C_{bw}, and C_{bca} versus effective pressure, normalized by C_s. Note in (2.4)–(2.5) that, unlike the C_{bca} coefficient, the other two compressibilities do not depend explicitly on P_{ca}. The nonlinear decreasing behavior observed in all the cases can be attributed to the closure of microcracks, low aspect ratio pores, and loose grain contacts, which increase the stiffness of the rock. In Fig. 3(b), we observe the variation of C_{bca} versus nonwetting saturation for a given wetting fluid pressure. The magnitude of this coefficient suggests that capillary pressure changes may have a non-negligible influence on bulk volume changes, particularly in the range of intermediate to high nonwetting saturations and for abnormally high pore pressures (low effective pressures).

C. Poroviscoelastic moduli

In the previous sections we considered bulk effective pressures and compressibilities, using purely elastic approximations of the elastic moduli. This approach is frequently used in many static or quasistatic problems in rock mechanics, which can be regarded as reversible processes. However, when considering dynamic problems such as wave propagation, the irreversible character of the deformation process plays a very important role.

The dissipation due to a viscous solid–fluid interaction was already introduced in the equations of motion with the terms d_n, d_w, and d_{nw}. In addition, as stated in Sec. III, viscoelastic dissipation must be incorporated in the formulation. The theoretical basis for the extension of the poroelastic formulation to include viscoelasticity were given by Biot[34,3] and later applied by different authors.[35–38] Using principles of irreversible thermodynamics, Biot established a general correspondence rule that allows us to extend our formulation to the poroviscoleastic case, replacing the real elastic coefficients by complex frequency-dependent moduli in the frequency domain.

Many mechanisms and models are proposed in the literature to explain the irreversible behavior observed in real rocks.[39] However, for practical purposes, we use the phenomenological model defined by Liu *et al.*[40] to describe attenuation by making the shear and undrained modulus complex and frequency dependent, while all the other coefficients remain real. This is a linear and causal model, whose associated complex modulus behaves properly in all the frequency range, and satisfies the restrictions imposed by the laws of thermodynamics.[41]

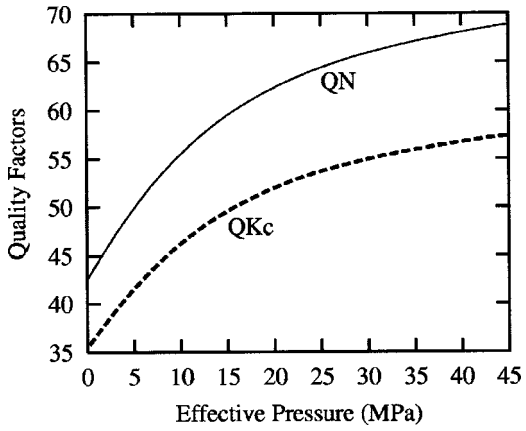

FIG. 4. Assumed values for $\hat{Q}_{Kc}$ and $\hat{Q}_N$ coefficients versus effective pressure.

Using this model, the complex moduli K_c, N are computed as

$$K_c(\omega, P_{\text{ef}}^b, \overline{S_n}) = \frac{K_c^r(P_{\text{ef}}^b, \overline{S_n})}{R_{K_c}(\omega, P_{\text{ef}}^b) - iT_{K_c}(\omega, P_{\text{ef}}^b)},$$
$$N(\omega, P_{\text{ef}}^b) = \frac{N^r(P_{\text{ef}}^b)}{R_N(\omega, P_{\text{ef}}^b) - iT_N(\omega, P_{\text{ef}}^b)}. \tag{4.14}$$

The real coefficients $K_c^r(P_{\text{ef}}^b)$ and $N^r(P_{\text{ef}}^b)$ denote the relaxed closed bulk and shear moduli, respectively. They are chosen so that the high-frequency limits of (4.14) match the values of $N(P_{\text{ef}}^b)$ and $K_c(P_{\text{ef}}^b, \overline{S_n})$ obtained from the experimental law (4.1) and (3.3), respectively. The frequency-dependent functions R_l and T_l, $l = K_c$, N, associated with a continuous spectrum of relaxation times, characterize the viscoelastic behavior and are given by[40,42]

$$R_l(\omega, P_{\text{ef}}^b) = 1 - \frac{1}{\pi \hat{Q}_l(P_{\text{ef}}^b)} \ln \frac{1 + \omega^2 T_{1,l}^2}{1 + \omega^2 T_{2,l}^2}, \tag{4.15}$$

$$T_l(\omega, P_{\text{ef}}^b) = \frac{2}{\pi \hat{Q}_l(P_{\text{ef}}^b)} \tan^{-1} \frac{\omega(T_{1,l} - T_{2,l})}{1 + \omega^2 T_{1,l} T_{2,l}}, \quad l = K_c, N. \tag{4.16}$$

The parameters $\hat{Q}_l$, $T_{1,l}$, and $T_{2,l}$ are taken such that the resulting quality factor $Q_l = T_l / R_l$ is approximately equal to $\hat{Q}_l$ in the range of frequencies where the equations are solved. For this computation we also introduced the dependence of the quality factors associated to K_c and N (i.e., $\hat{Q}_{Kc}$ and $\hat{Q}_N$), on effective pressure,[43] disregarding any possible dependence of such coefficients on saturation. The corresponding curves are shown in Fig. 4.

D. Wave velocities

We apply the formulation described in Sec. III to analyze the phase velocities [given by (3.6)] versus effective pressure and saturation, in the ultrasonic frequency range ($f = 1$ MHz) commonly used in laboratory experiments.

Figure 5(a) shows the well-known behavior of the type-I P-and S-wave velocities, which have a marked increase with increasing effective pressure.[8,44,47] Figure 5(b) shows the type-I P-wave velocity versus saturation for $\overline{P_w} = 45$ MPa (that is, for an excess wetting fluid pressure $\Delta P_{wh} \simeq 16$ MPa). As expected, there is a maximum at minimum oil saturation, and a decreasing trend at intermediate states. The absolute minimum corresponds to the effect observed in the effective pressure law near the residual brine saturation [see Fig. 1(b)].

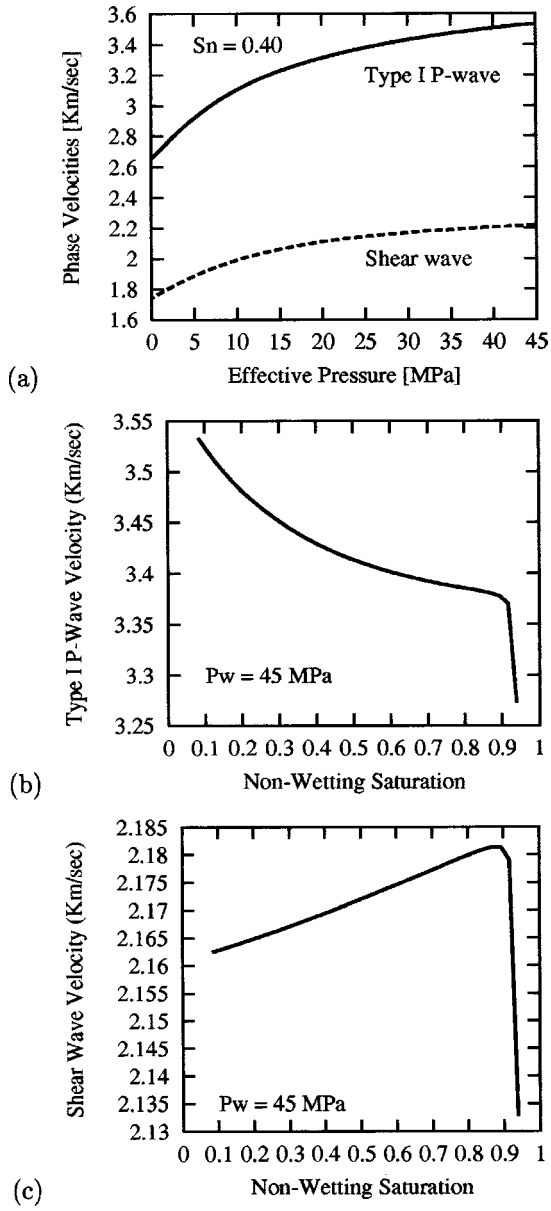

FIG. 5. Type I P- and S-wave phase velocities versus effective pressure (a), and versus nonwetting fluid saturation [(b) and (c)].

The shear wave velocity, shown in Fig. 5(c) increases almost linearly with increasing oil saturation, showing the same abrupt decrease associated with the anomaly of the effective pressure near $\overline{S_n} = 1 - S_{rw}$. Except at this point, the changes are only associated with density effects, since the bulk density [given by (3.2)] decreases with increasing $\overline{S_n}$ and by hypothesis the matrix shear modulus does not depend on saturation.

In Fig. 6(a), we plot the type-II and type-III P-wave

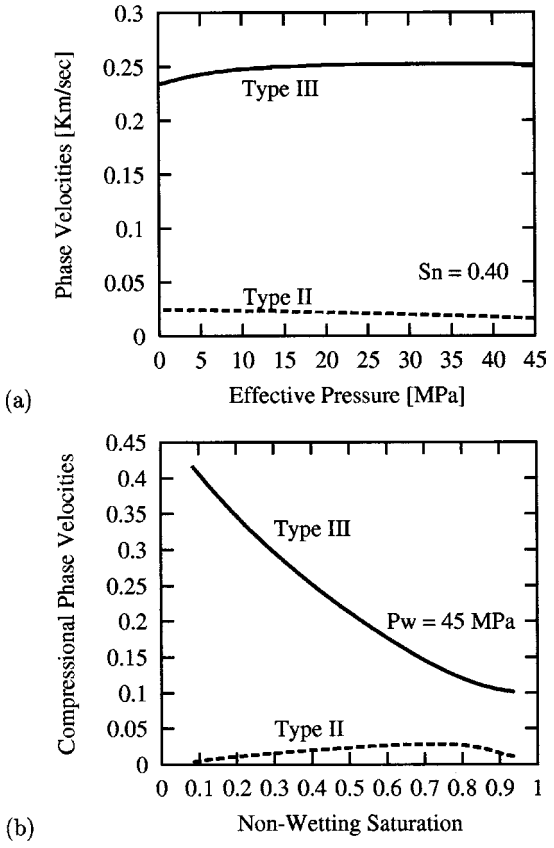

FIG. 6. Type-II and type-III P-wave phase velocities versus effective pressure (a), and versus nonwetting fluid saturation (b).

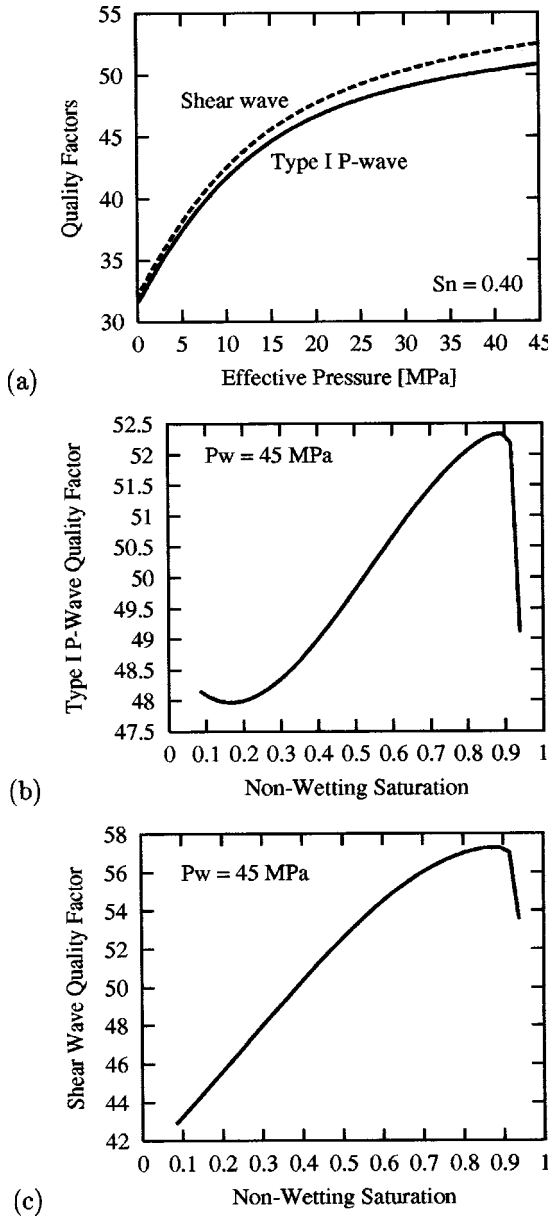

FIG. 7. Type-I P- and S-wave quality factors versus effective pressure (a), and versus nonwetting fluid saturation [(b) and (c)].

velocities versus effective pressure, which are almost constant in the whole pressure range. Figure 6(b) shows the phase velocities versus saturation. We observe for this sandstone that the type-III P wave is very sensitive to oil saturation. The velocity of the type-II P wave has a maximum at intermediate saturation values, approaching zero near the residual saturations. This suggests that the mobility of the fluid phases plays an important role. The behavior of these velocities versus frequency was analyzed by Santos *et al.*[10] using a poroelastic formulation.

E. Quality factors

We use Eq. (3.6) to compute the quality factors Q_{I}, Q_{II}, Q_{III}, and Q_{S} associated with the different wave modes. The quality factors of the type-I P and S waves are shown in Figs. 7(a), (b), and (c). They show a pronounced monotonic increase with increasing effective pressure, in agreement with the observations made by different authors in other sandstones.[15,16,44.47]

The behavior of Q_{I} versus saturation is more complex, showing a relative minimum in the range from low to intermediate nonwetting (oil) saturation. The shear-wave quality factor Q_{S} tends to increase with oil saturation. Since an increase in oil saturation increases the viscosity of the fluid mixture—and hence the viscous dissipation—these results suggest a nonlinear relationship between quality factors and viscosities showing the influence of viscous and inertial forces. This behavior was also observed when using a simple isostress mixture model (i.e., with zero capillary forces), as described in Berryman *et al.*[7] Both quality factors show an abrupt decrease near the irreducible brine saturation, as can be appreciated in the corresponding wave velocities.

To our knowledge, no laboratory or field data of attenuation versus saturation for water–oil saturated sandstones are available. However, we can compare the predictions of our model with the observations made by different researchers in water–air (or water–gas) saturated rocks, considering water as the wetting phase. A careful analysis of the results published by Murphy III[45] for Massilon sandstone, of the averages obtained by Jones *et al.*[46] using a set of nine sandstones, and of the discussion in Schön[47] (Sec. 7.3.4.1), allows us to conclude that Q_{S} increases with $\overline{S_n}$, and that Q_{I} has a minimum at intermediate saturation states.

The quality factors for type-II and type-III compressional waves are shown in Figs. 8(a) and (b). Although they

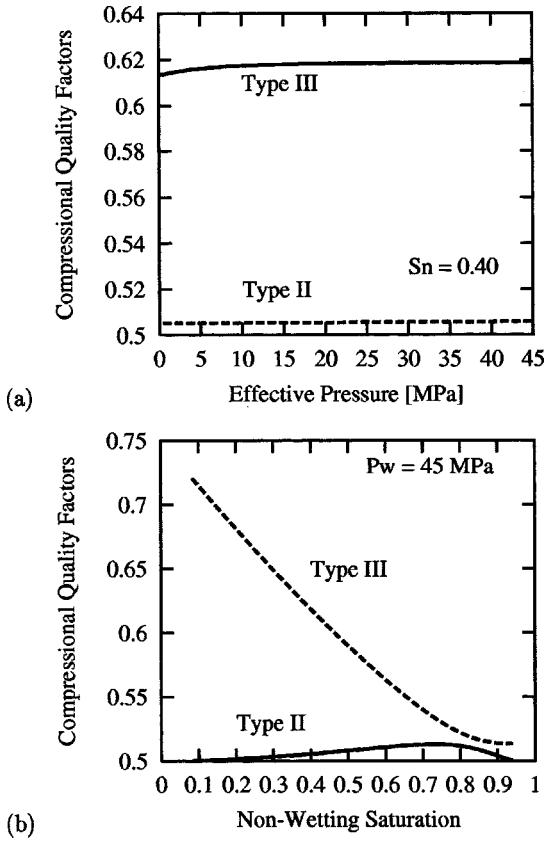

FIG. 8. Type-II and type-III P-wave quality factors versus effective pressure (a), and versus nonwetting fluid saturation (b).

are not very sensitive to effective pressure, they show appreciable variations in the whole saturation range.

V. CONCLUSIONS, REMARKS, AND FUTURE WORK

We have investigated the effects of effective pressure and fluid saturation on different static and dynamic properties of reservoir rocks. We have analyzed the behavior of a hydrocarbon (oil–brine) transition zone in a well consolidated sandstone, incorporating a realistic capillary pressure curve. The computations include the estimation of bulk volume compressibilities, effective pressure, ultrasonic phase velocities, and quality factors of the different wave modes, under different fluid pressures and saturations. Our main results can be summarized as follows.

(1) The effective pressure versus saturation curve is almost constant, showing an abrupt decrease near the maximum admissible value of the nonwetting saturation (i.e., the irreducible brine saturation). Such a decrease is reflected in both the fast P- and S-wave velocities and quality factors. Unfortunately, nothing can be concluded from the available published data, since it requires detailed information about the fluid pressure conditions during the experiments.

(2) For normal–hydrostatic–to intermediate wetting fluid pressures, the results obtained with classical formulas for the effective pressure (such as the differential pressure law of Gangi–Carlson[31]), may differ substantially from our estimations. For highly overpressured reservoirs (high $\overline{P_w}$, low P_{wd}), however, the differential pressure of the wetting phase gives a good estimate of the effective pressure, extending a result valid also for single-phase fluid saturated rocks.[31]

(3) The behavior of the bulk compressibilities versus effective pressure are similar to those observed in fully saturated rocks, and are controlled by the decrease of the matrix compressibility with pressure. In particular, it must be noted the magnitude of the new compressibility C_{bca}, indicating the influence that capillary pressure variations may have on bulk volume changes. This is particularly important in the range of intermediate to high nonwetting saturations, and for abnormally high pore pressures (low effective pressures).

(4) Regarding the type-I (fast) P and S waves, our model simulates the increase in velocities and quality factors with effective pressure observed in laboratory experiments. Consequently, these quantities can be good indicators of abnormally high fluid pressures.
The behavior of Q_I and Q_S for variable nonwetting (oil) saturation is, in general, coherent with observations made in similar situations (except at the residual brine saturation), and was also verified using an isostress mixture model for the fluids. Our results suggest that, unlike the corresponding phase velocity, the shear wave quality factor can be a good fluid indicator, particularly for normal (hydrostatic) to intermediate pressure conditions.

(5) The velocities and quality factors of the type-II and type-III compressional waves are not very sensitive to pressure variations, but show a strong dependence on saturation.

(6) The influence of capillary pressure on the acoustic properties of the different wave modes, was analyzed by comparing our results with the simplified isostress model—analogous to Biot's classical theory, in which only type-I, type-II P and S waves can propagate. We observe that, except at the irreducible brine saturation (where capillary pressure reaches its maximum), there is almost no difference between type-I P- and S-wave velocities. For type-II P waves, however, important differences can be observed. This seems reasonable since the first two waves involve coupled solid–fluid motions, while the latter is affected by the fluid mobility. Appreciable differences are observed in the quality factors given by the two models, indicating that the quality factors are more sensitive to capillary pressure than the phase velocities. This suggests that quality factor analysis can be used as a tool for discriminating full saturation from two-phase or partial saturation.

We must point out some limitations of the model, since due to the lack of data, we ignored the possible dependence of frame moduli with capillary pressure, an effect that should be carefully investigated. The same holds for the coefficients $\hat{Q}_{Kc}$ and $\hat{Q}_N$, which for simplicity were taken independent of saturation. We also neglected the variations of petrophysical quantities such as porosity and permeability with effective pressure. Consequently, these results should be compared to appropriate laboratory experiments or field data.

Moreover, since unconsolidated reservoir sandstones are expected to show large sensitivity to fluid type and effective pressure,[33] a similar theoretical and applied analysis should be performed for such cases.

Finally, a rock in the subsurface is subjected to a nonhydrostatic state of stress: in general, the vertical stress is greater than the horizontal stress, and this situation induces P- and S-wave anisotropy in an otherwise isotropic rock.[48] Therefore, the theory should be generalized to describe anisotropy, and its related pressure effects.

ACKNOWLEDGMENTS

This work was funded by the Agencia Nacional de Promoción Científica y Tecnológica, Argentina (Contract No. BID-802/OC-AR), the European Union under the project ''Detection of overpressured zones from seismic and well data'' and CONICET, Argentina (PIP 0363/98).

[1] M. A. Biot, ''Theory of propagation of elastic waves in a fluid-saturated porous solid. I. Low frequency range,'' J. Acoust. Soc. Am. **28**, 168–171 (1956).
[2] M. A. Biot, ''Theory of propagation of elastic waves in a fluid-saturated porous solid. II. High frequency range,'' J. Acoust. Soc. Am. **28**, 179–191 (1956).
[3] M. A. Biot, ''Mechanics of deformation and acoustic propagation in porous media,'' J. Appl. Phys. **33**, 1482–1498 (1962).
[4] N. C. Dutta and H. Odé, ''Attenuation and dispersion of compressional waves in fluid-filled porous rocks with partial gas saturation (White model)—Part I: Biot theory,'' Geophysics **44**, 1777–1788 (1979).
[5] J. E. White, ''Computed seismic speed and attenuation in rocks with partial gas saturation,'' Geophysics **40**, 224–232 (1975).
[6] S. Mochizuki, ''Attenuation in partially saturated rocks,'' J. Geophys. Res. **87**, 8598–8604 (1982).
[7] J. Berryman, L. Thigpen, and R. Chin, ''Bulk elastic wave propagation in partially saturated porous solids,'' J. Acoust. Soc. Am. **84**, 360–373 (1988).
[8] M. N. Toksöz, C. H. Cheng, and A. Timur, ''Velocities of seismic waves in porous rocks,'' Geophysics **41**, 621–645 (1976).
[9] J. E. Santos, J. Douglas, Jr., J. M. Corberó, and O. M. Lovera, ''A model for wave propagation in a porous medium saturated by a two-phase fluid,'' J. Acoust. Soc. Am. **87**, 1439–1448 (1990).
[10] J. E. Santos, J. M. Corberó, and J. Douglas, Jr., ''Static and dynamic behavior of a porous solid saturated by a two-phase fluid,'' J. Acoust. Soc. Am. **87**, 1428–1438 (1990).
[11] J. M. Carcione and U. Tinivella, ''Bottom-simulating reflectors: seismic velocities and AVO effects,'' Geophysics **65**, 54–67 (2000).
[12] U. Tinivella and J. M. Carcione, ''Estimation of gas–hydrate concentration and free-gas saturation from log and seismic data,'' The Leading Edge **20**, 200–203 (2001).
[13] *Advances in Porous Media*, edited by M. Yavuz Corapcioglu (Elsevier, Amsterdam, 1996).
[14] H. B. Helle, ''Detection of overpressure zones from seismic and well data, A summary of activities,'' Norsk Hydro Report No. R-089689, Norsk Hydro E & P Research Centre, N-5020 Bergen, Norway, 1999.
[15] J. M. Carcione and A. Gangi, ''Gas generation and overpressure: effects on seismic attributes,'' Geophysics **65**, 1769–1779 (2000).
[16] J. M. Carcione and A. Gangi, ''Non-equilibrium compaction and abnormal pore-fluid pressures: effects on rock properties,'' Geophys. Prospect. **48**, 521–537 (2000).
[17] M. S. King, ''Wave velocities in rocks as a function of changes in overburden pressure and pore fluid saturants,'' Geophysics **31**, 50–73 (1966).
[18] J. Bear, *Dynamics of Fluids in Porous Media* (Dover, New York, 1972).
[19] R. E. Collins, *Flow of Fluids Through Porous Materials* (Reinhold, New York, 1961).
[20] A. Scheidegger, *The Physics of Flow Through Porous Media* (MacMillan Company, Toronto, 1974).
[21] D. W. Peaceman, *Fundamentals of Numerical Reservoir Simulation* (Elsevier, Amsterdam, 1977).
[22] R. W. Zimmerman, *Compressibility of Sandstones* (Elsevier Science, Amsterdam, 1991).
[23] About the differences in notation between this paper and the former (Ref. 10), it must be mentioned that the old variables ΔP, S_0, and e now correspond to ΔP_c, S_n, and e_b.
[24] J. L. Auriault, O. Lebaigue, and G. Bonnet, ''Dynamics of two immiscible fluids flowing through deformable porous media,'' Transp. Porous Media **4**, 105–128 (1989).
[25] J. E. Santos, J. M. Corberó, C. L. Ravazzoli, and J. L. Hensley, ''Reflection and transmission coefficients in fluid saturated porous media,'' J. Acoust. Soc. Am. **91**, 1911–1923 (1992).
[26] F. Gassmann, ''Über die elastizitat poröser mediem,'' Vierteljahrsschr Naturforsch. Ges. Zurich **96**, 1–23 (1951).
[27] R. L. Mann and I. Fatt, ''Effect of pore fluids on the elastic properties of sandstone,'' Geophysics **25**, 433–444 (1960).
[28] J. Douglas, Jr., J. L. Hensley, and P. J. Paes Leme, ''A study of the effect of inhomogeneities on immiscible flow in naturally fractured reservoirs,'' *International Series of Numerical Mathematics* (Birkhauser-Verlag, Basel, 1993), Vol. 114, pp. 59–74.
[29] J. Berryman, ''Elastic wave propagation in fluid-saturated porous solids,'' J. Acoust. Soc. Am. **69**, 416–424 (1981).
[30] J. M. Hovem and G. D. Ingram, ''Viscous attenuation of sound in saturated sand,'' J. Acoust. Soc. Am. **66**, 1807–1812 (1979).
[31] A. F. Gangi and R. L. Carlson, ''An asperity-deformation model for effective pressure,'' Tectonophysics **256**, 241–251 (1996).
[32] C. L. Ravazzoli and J. E. Santos, ''Compressibility analysis of Berea sandstone versus saturation and effective pressure,'' *EAGE 62nd Conference and Technical Exhibition*, Glasgow, 29 May–2 June 2000, Extended Abstracts Book, Paper D-36, 2000.
[33] R. Guerra, J. Meyer, A. Sibbit, and R. Van Delden, ''Integrated time-lapse rock physics measurements—the key to understanding reservoir elastic moduli changes with hydrocarbon production,'' *Proceedings of PARIS 2000, Petrophysics Meets Geophysics*, 2000, Paper A-2.
[34] M. A. Biot, ''Theory of deformation of a porous viscoelastic anisotropic solid,'' J. Appl. Phys. **27**, 459–467 (1956).
[35] R. D. Stoll, ''Acoustic waves in saturated sediments,'' in *Physics of Sound in Marine Sediments*, edited by L. Hampton (Plenum, New York, 1974), pp. 19–39.
[36] R. D. Stoll and G. M. Bryan, ''Wave attenuation in saturated sediments,'' J. Acoust. Soc. Am. **47**, 1440–1447 (1970).
[37] J. D. Keller, ''Acoustic wave propagation in composite fluid-saturated media,'' Geophysics **54**, 1554–1563 (1989).
[38] P. Rasolofosaon, ''Plane acoustic waves in linear viscoelastic porous media: energy, particle displacement and physical interpretation,'' J. Acoust. Soc. Am. **89**, 1532–1550 (1991).
[39] *Seismic Wave Attenuation*, edited by M. Nafi Toksöz and D. Johnston, Geophysics Reprint Series No. 2, Society of Exploration Geophysicists, 1981.
[40] H. P. Liu, D. L. Anderson, and H. Kanamori, ''Velocity dispersion due to anelasticity; implications for seismology and mantle composition,'' Geophys. J. R. Astron. Soc. **47**, 41–58 (1976).
[41] C. L. Ravazzoli, ''Modelling of wave propagation phenomena in dissipative media,'' Ph.D. Thesis, Facultad de Ciencias Astronómicas y Geofísicas, Universidad Nacional de La Plata, Argentina, 1995 (in Spanish).
[42] J. M. Carcione, *Wave Fields in Real Media: Wave Propagation in Anisotropic, Anelastic and Porous Media* (Pergamon, Amsterdam, 2001).
[43] K. Winkler and A. Nur, ''Pore fluids and seismic attenuation in rocks,'' Geophys. Res. Lett. **6**, 1–4 (1979).
[44] G. Tao, M. S. King, and M. Nabi-Bidhendi, ''Ultrasonic wave propagation in dry and brine-saturated sandstones as a function of effective stress: laboratory measurements and modelling,'' Geophys. Prospect. **43**, 299–327 (1995).
[45] W. F. Murphy III, ''Effects of partial water saturation on attenuation in Massilon sandstone and Vycor porous glass,'' J. Acoust. Soc. Am. **71**, 1458–1468 (1982).
[46] S. Jones, T. Astin, and C. Mc Caan, ''The effect of degree of saturation on ultrasonic velocity and attenuation in sandstones,'' *Annual Meeting Abstracts*, Society of Exploration Geophysicists, pp. 1023–1026.
[47] J. H. Schön, *Physical Properties of Rocks: Fundamentals and Principles of Petrophysics*, Handbook of Geophysical Exploration (Elsevier Science, Amsterdam, 1996), Vol. 18.
[48] J. M. Carcione, ''Energy balance and fundamental relations in dynamic anisotropic poroviscoelasticity,'' Proc. R. Soc. London, Ser. A **457**, 331–348 (2000).